Potentiostatic Infrared Titration of 11-Mercaptoundecanoic Acid Monolayers

Antonio M. Luque,[a] *Angel Cuesta,*[b,c] *Juan José Calvente* [a] *and Rafael Andreu* [a,*]

[a] Departamento de Química Física. Universidad de Sevilla. 41012-Sevilla, Spain

[b] Instituto de Química Física "Rocasolano", CSIC, 28006-Madrid, Spain

[c] Present address: Department of Chemistry, School of Natural and Computing Sciences,
University of Aberdeen, Aberdeen AB24 3UE, UK

[*] Corresponding author: Phone: +34-954557177, Fax: +34-954557174, E-mail: fondacab@us.es

Abstract

In situ IR difference spectra of 11-mercaptoundecanoic acid (MUA) monolayers deposited on gold, and in the presence of a NaF solution in deuterated water, have been recorded as a function of both solution pH^* and substrate's potential. IR spectra recorded under voltammetric conditions indicate that the potential-induced ionization of the monolayer is a slow process, involving a simultaneous rearrangement of the hydrocarbon chains, and that a significant population of carboxylic groups are not dissociated at positive potentials, even in the presence of a pH^* 9 solution. Steep potentiostatic IR titration curves, consistent with a monolayer $pK_a = 4.3$, are obtained at negative potentials. As the potential is made more positive, titration curves become lower, broader and are shifted towards more basic pHs, as would be expected when only a fraction of the carboxylic groups become ionized in the presence of less favorable interactions. Rather than acting directly on the electrostatic energy of the carboxylate groups, the electrode potential seems to control the ionization of the monolayer by attracting (or repelling) cations from the electrolyte and by reorienting the thiol head groups inside and outside the low permittivity layer of methylene chains.

Keywords: Acid monolayers, ATR-SEIRAS, potential-induced reorientation, potential-induced proton transfer.

1. Introduction

Gold surfaces modified with monolayers of ω-mercaptoalkanoic acids display acid/base properties that have found a variety of applications, such as anchoring biomolecules [1-4] or modulating surface wettability [5-7]. External control of the monolayer ionization constitutes a key aspect of these applications. Usually, this control is exerted through the solution pH, but attachment of the thiol group to a metallic substrate opens the possibility of applying a potentiostatic control on the ionization degree of the terminal carboxylic groups. Evidence supporting the influence of the substrate potential on the acid dissociation of thiol monolayers has been gathered from a variety of techniques, including voltammetric [8-12], surface Raman [13], quartz microbalance [14] and infrared absorption [15,16] experiments. These results can be classified into two groups. The first group [8-13] displays an increase of the monolayer acidity as the potential is made more positive (in agreement with predictions from electrostatic models [17-19]), whereas the second group [14-16] shows the opposite trend (which has been rationalized in terms of a cation-exchange model [14-15]). The potential-induced ionization of 11-mercaptoundecanoic acid (MUA) monolayers has been reported to display both of these opposite trends, under the scrutiny of different experimental techniques and in the presence of different electrolyte solutions. In this work, we have used surface-enhanced infrared absorption spectroscopy to assess *in situ* the changes undergone by a MUA monolayer deposited on gold when both the substrate potential and the solution pH are varied. To obtain potentiostatic IR titration curves, we have implemented a new protocol that provides direct comparison of the same monolayer at any available potential and pH with its (mostly) non-ionized state in acid solution. Simultaneous observation of the methylene, carbonyl and carboxylate stretching modes of the thiol monolayer shows that potential-induced ionization is a slow process, involving a reorientation of the alkyl chains, and that deprotonation shifts towards more basic solutions as the potential is made more positive.

2. Material and methods

Deuterium oxide (99.9%) and 11-Mercaptoundecanoic acid (95%) were purchased from Sigma-Aldrich. Sodium deuteroxide (40%) was from Fluka, both absolute ethanol and perchloric acid (70%) were from Merck, and Puratronic sodium fluoride of high purity was from Alfa Aesar. Water was purified with a Millipore Milli-Q system (resistivity 18 MΩ cm).

The ATR spectroelectrochemical set-up and the procedure to prepare the gold film on a silicon substrate have been described previously [20]. To modify the working electrode, the gold film was kept in contact with an ethanolic solution of 1 mM 11-mercaptoundecanoic acid for 48 hours. The modified surface was then carefully cleaned with absolute ethanol and deuterated water. A glass electrode was inserted in the cell for continuous monitoring of the solution acidity. The glass electrode was calibrated with standard H_2O solutions, and its reading in the D_2O working solutions was reported as pH^* values, which are related to conventional pH values by $pH = 0.936\ pH^* + 0.412$ [21]. Experiments were carried out at room temperature.

ATR-SEIRAS spectra were recorded with a Nicolet 6700 FTIR spectrometer, and all experiments were carried out with *p*-polarized light. Difference spectra were computed from the sample and reference reflectivities, R and R_{ref} respectively, and they were displayed as plots of $\text{Absorbance} = -\log(R/R_{ref})$ vs. wavenumber of the IR radiation.

3. Results and Discussion

Some key aspects of the potential-induced ionization of the MUA monolayer can be easily observed by recording the IR spectra under slow ($v = 5$ mV s^{-1}) voltammetric conditions in the presence of an alkaline solution, where carboxylic groups are expected to be dissociated. To this end, the spectroelectrochemical cell was filled with a 5 mM NaF solution of pH^* 9 in deuterated water, whose composition was intended to avoid spectral interferences from the electrolyte. Starting at 0.3 V, the potential was initially scanned towards more negative values, and the scanning direction was eventually reversed after reaching a minimum potential of -0.7 V. Difference spectra recorded at some representative potential values along the cyclic scan are displayed in Figure 1. We have focused on five bands that are directly related to MUA vibration modes, namely: (i) the methylene asymmetric and symmetric stretchings at 2920 cm^{-1} and 2840 cm^{-1}, respectively, (ii) the carbonyl band of the carboxylic group at 1690 cm^{-1}, and (iii) the carboxylate asymmetric and symmetric stretchings at 1550 cm^{-1} and 1410 cm^{-1}, respectively [15,16,22-24]. As the potential is made more negative, the two carboxylate bands in Figure 1b at 1550 cm^{-1} and 1410 cm^{-1} increase and, simultaneously, the band at 1690 cm^{-1} decreases to a similar extent, indicating a potential-induced ionization of the carboxylic groups that are present in the monolayer at 0.3 V, where the reference spectrum was recorded. A less obvious result is the concomitant decrease in Figure 1a of the two methylene bands at 2920 cm^{-1} and 2840 cm^{-1}. Since the number of methylene groups remains invariant in these experiments, it seems reasonable to assign the decrease in their band intensities to a change in the orientation of their transition dipole moments. Allara et al. [25,26] have shown that the intensities of the two CH_2 stretching bands decrease when the hydrocarbon chain reorients towards the surface normal, thereby making the orientation of the corresponding transition dipole moments more parallel to the metal surface. According to this interpretation, the hydrophilic carboxylate heads would reorient the hydrocarbon chain of the chemisorbed thiols by pulling them towards the solution. It should be pointed out that similar potential-induced reorientations have been proposed by Uosaki et al. [27] and Burgess et al. [28] to account for the changes brought into the IR spectrum of electroactive SAMs upon oxidizing their redox moieties.

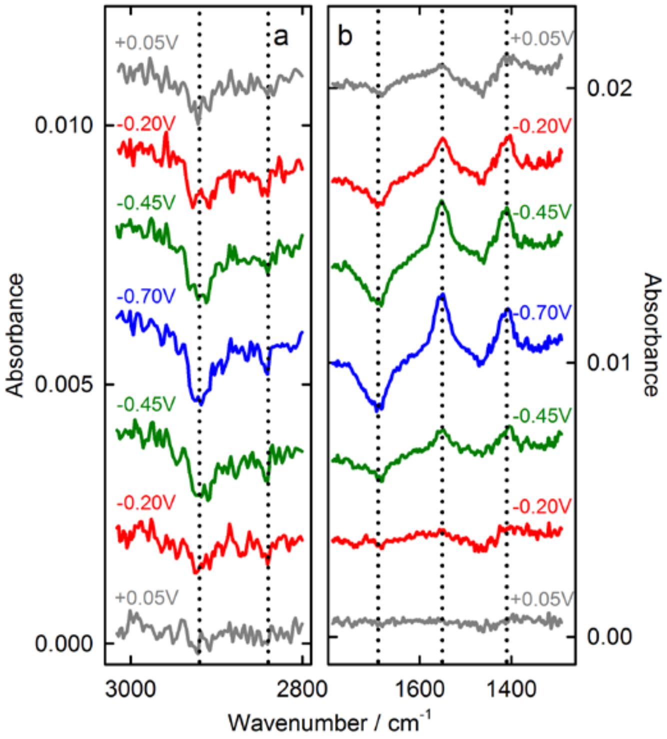

Figure 1. (a) Methylene and (b) carboxylic/carboxylate bands of difference IR spectra of a MUA SAM in contact with a 5 mM NaF (pH* 9) solution in D_2O recorded while the potential was being scanned at 5 mV s^{-1}. Starting from the bottom, the potential was first swept in the negative direction, and then the sweep direction was reversed upon reaching -0.7 V. The reference spectrum was recorded at 0.3 V. Dotted vertical lines help to locate the following wavenumbers: 2920, 2840, 1690, 1550 and 1410 cm^{-1}. Spectra have been shifted vertically for clarity.

By comparing the band intensities at the same potential in the forward and reverse scans, it becomes evident that the ionization of the monolayer is significantly delayed with respect to the potential perturbation. This hysteresis varies somewhat along the scan, amounting to as much as 1 min at intermediate potentials, and it implies a slow ionization and reorganization of the adsorbed thiol molecules as a response to changes in the applied potential.

To obtain potentiostatic titration curves of the same monolayer under equilibrium conditions, we used as a reference the (nearly) neutral monolayer in contact with an acid solution of pH* 3.4 [29], and varied both potential and pH* according to the sequence illustrated in Figure 2.

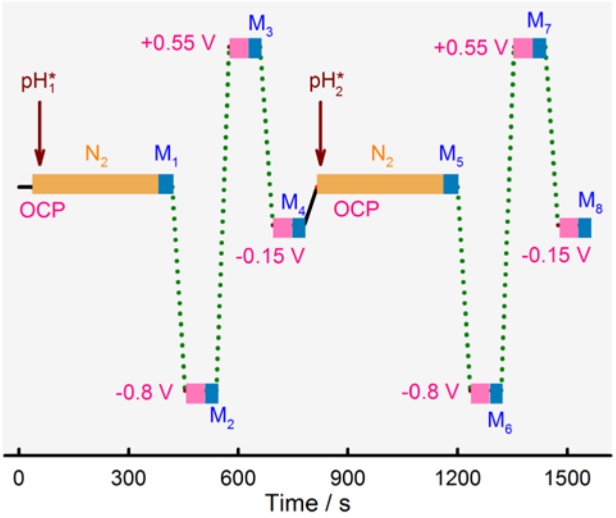

Figure 2. Temporary sequence of the solution pH* and electrode potential variations for monolayer titration at -0.8 V, +0.55 V and -0.15 V, and at open circuit potential (OCP). Vertical arrows indicate NaOD additions to the cell solution. Orange bars indicate waiting times with nitrogen bubbling through the solution. Pink bars indicate 1 min waiting time to equilibrate the monolayer at the specified potential. Blue bars and M_i symbols stand for measurement of the i-th infrared spectrum.

The three potential values were chosen to lie on both sides and in the middle of the potential of zero charge interval of MUA monolayers deposited on Au(111) that were exposed to similar pH variations [30]. Initially, reference spectra at each potential and at open circuit were recorded in the presence of the pH* 3.4 solution. Then, a few microliters of a 10^{-3} M NaOD solution were added to the cell solution to increase its pH* and the spectra corresponding to open circuit and the three selected potentials were recorded, after applying a waiting time of 1 min in each case to allow for monoloyer equilibration at each new potential. This procedure was then repeated after successive additions of the NaOD solution.

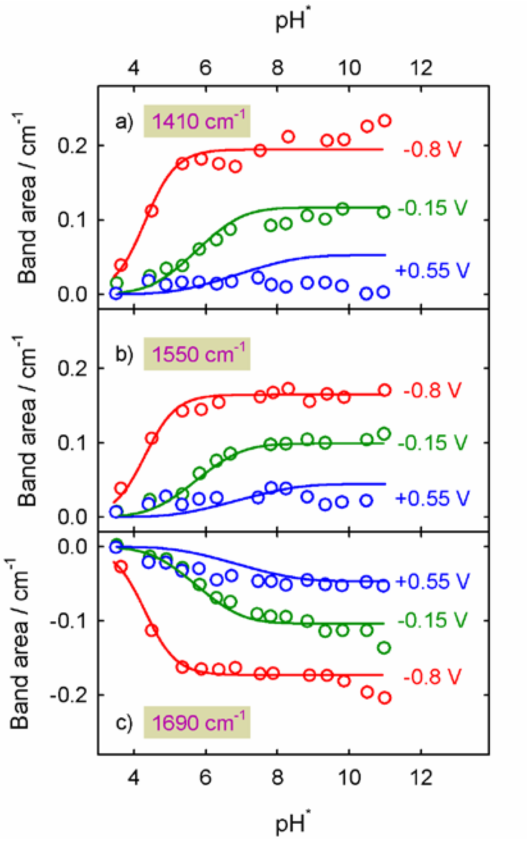

Figure 3. Integrated intensities of the a) 1550 cm^{-1}, b) 1410 cm^{-1} and c) 1690 cm^{-1} bands at the indicated potentials as a function of the solution pH*. Reference spectra at each potential were initially recorded in the pH* 3.4 solution. Solid lines were computed from eq (3) in the text.

Steep titration curves for the integrated IR bands are observed in Figure 3 at the most negative potential (-0.8 V), but band areas become significantly smaller at any pH^* as the potential is made more positive. This decrease in band area may be due to an incomplete ionization of the monolayer or to a potential-induced reorientation of the carbonyl and carboxylate groups. This last explanation is not likely to apply for the IR bands recorded at -0.15 V, since the three band areas at -0.8 V and -0.15 V retain their relative magnitude in the basic $8 \leq pH^* \leq 11$ range, and a potential-induced reorientation is not expected to affect to the same extent to the stretching bands of the neutral carbonyl and the charged carboxylate groups, whose transition dipoles point to different directions with respect to the molecular backbone. On the other hand, the incomplete ionization hypothesis is in agreement with our previous observation in Figure 1 of a significant population of carbonyl groups at 0.3 V and pH^* 9, and it implies that some carboxylic groups cannot be ionized up to pH^* 13, possibly because they become buried into the layer of methylene chains at positive potentials [31]. The trend towards a lower ionization at more positive potentials extends also to the spectra recorded at 0.55 V, but now the carbonyl band area is about five times bigger than any of the two carboxylate band areas. This disparity in the carboxylate and carbonyl band areas points to a potential-induced reorientation of the carboxylate group, so that the O-C-O plane and, therefore, the IR transition dipoles of the symmetric and asymmetric carboxylate stretchings become nearly parallel to the metal surface at the most positive potential. Band areas recorded under OCP conditions (not shown in Figure 3 for clarity) displayed intermediate values between those obtained at 0.55 V and -0.15 V, and were compared with those obtained in independent OCP titrations as a check of the monolayer integrity while the potential was being varied within a large polarization window.

Titration curves become also shifted toward higher pH* values when the potential is made more positive, as it would be expected when repulsive interactions between carboxylate anions hinder a further ionization of the monolayer. This effect can be discussed in terms of the following expression [32]:

$$\mathrm{pH}^* - \mathrm{p}K_\mathrm{a} = \log \frac{\Gamma_{ROO^-} / \Gamma_{ROO^-}^{max}}{1 - \dfrac{\Gamma_{ROO^-}}{\Gamma_{ROO^-}^{max}}} + \alpha \cdot \frac{\Gamma_{ROO^-}}{\Gamma_{ROO^-}^{max}} \tag{1}$$

where K_a is the intrinsic dissociation equilibrium constant, Γ_{ROO^-} is the surface concentration of carboxylate groups, $\Gamma_{ROO^-}^{max}$ is the maximum surface concentration of carboxylic groups that can be ionized at a given potential and α is a mean field interaction parameter that accounts for the electrostatic interactions between carboxylate anions. Assuming that all $\Gamma_{ROO^-}^{max}$ groups become ionized for pH* > 10, the following relationship holds between the absorbance A and the $\Gamma_{ROO^-} / \Gamma_{ROO^-}^{max}$ ratio:

$$\mathrm{A}_{\mathrm{E,pH*}} = \mathrm{A}_{\mathrm{E,pH*>10}} \frac{\Gamma_{COO^-}}{\Gamma_{COO^-}^{max}} \tag{2}$$

so that eq (1) can be rewritten as:

$$\mathrm{pH}^* - \mathrm{p}K_\mathrm{a} = \log \frac{\mathrm{A}_{\mathrm{E,pH*}} / \mathrm{A}_{\mathrm{E,pH*>10}}}{1 - \dfrac{\mathrm{A}_{\mathrm{E,pH*}}}{\mathrm{A}_{\mathrm{E,pH*>10}}}} + \alpha \cdot \frac{\mathrm{A}_{\mathrm{E,pH*}}}{\mathrm{A}_{\mathrm{E,pH*>10}}} \tag{3}$$

Satisfactory fits of eq (3) to experimental titrations curves are obtained for the titrations at -0.8 V (with $\mathrm{pK_a} = 4.3$, $\alpha = 0$) and -0.15 V (with $\mathrm{pK_a} = 5.3$, $\alpha = 2$), but theoretical curves at 0.55 V (with $\mathrm{pK_a} = 6.0$, $\alpha = 4$) can only be considered as an indicative reference due to the consistently low values recorded at this potential. Assuming that extinction coefficients at the three wavelengths considered are independent of potential, the decrease of $\mathrm{A}_{\mathrm{E,pH*>10}}$ upon increasing the potential amounts to a decrease of $\Gamma_{ROO^-}^{max}$ according to a 1 : 0.47 : 0.27 ratio, so that most of the carboxylic groups are buried within the methylene chains and cannot be titrated at the most positive potentials. The carboxylic groups available for titration display higher pK_a and α values at positive potentials, as would be expected if ionization took place in an environment with a lower permittivity and stronger repulsive interactions between the carboxylate groups. Furthermore, cations attracted to the double layer at negative potentials will provoke an additional screening of the repulsive interactions between carboxylate groups, favoring deprotonation. Rather than acting directly on the electrostatic energy of the carboxylate groups, the electrode potential seems to control the ionization of the monolayer by attracting (or repelling) cations from the electrolyte and by reorienting the thiol head groups inside and outside the low permittivity layer of methylene chains.

4. Conclusions

In situ ATR-SEIRAS experiments provide straightforward evidence of the influence of potential on the ionization of 11-mercaptoundecanoic SAMs deposited on gold. Potential-induced ionization turns out to be a slow process, producing a delay of ~ 1 min between the IR signals recorded along forward and reverse voltammetric scans, and it involves a reorientation of the hydrocarbon chains towards a more upright orientation. Potentiostatic IR titration curves can be rationalized by assuming that negative potentials facilitate a close contact between immobilized carboxylates and electrolyte cations, thereby screening the negative charges of the carboxylate groups. At positive potentials, cations are repelled from the electrode and thiol head groups are attracted towards the metal and the hydrocarbon chains, leading to an energetically unfavorable scenario where ionization takes place in a low-permittivity environment and becomes further inhibited by the unscreened repulsion between carboxylate anions.

Acknowledgment

This work was supported by the Spanish DGICYT under grant CTQ2008-00371 and by the Junta de Andalucía under grant P07-FQM-02492.

References

(1) R. A. Clark, E. F. Bowden, Langmuir 13 (1997) 559-565.

(2) B. Jin, G. Wang, D. Millo, P. Hildebrandt, X. Xia, J. Phys. Chem. C 116 (2012) 13038-13044.

(3) H. Yue, D. H. Waldeck, J. Petrovic, R. A. Clark, J Phys Chem B 110 (2006) 5062-5072.

(4) G. A. Campbell, R. Mutharasan, Anal. Chem. 78 (2006) 2328-2334.

(5) J. Lahann, S. Mitragotri, T. Tran, H. Kaido, J. Sundaram, I. S. Choi, S. Hoffer, G. A. Somorjai, R. Langer, Science 299 (2003) 371-374.

(6) D. K. Peng, S. T. Yu, D. J. Alberts, J. Lahann, Langmuir (2007) 297-304.

(7) M. Luo, A. Amegashie, A. Chua, G. K. Olivier, J. Frechette, J. Phys. Chem. C 116 (2012) 13964-13971.

(8) H. S. White, J. D. Peterson, Q. Cui, K. J. Stevenson, J. Phys. Chem. B 102 (1998) 2930-2934.

(9) I. Burgess, B. Seivewright, R. B. Lennox, Langmuir 22 (2006) 4420-4428.

(10) S. M. Rosendahl, I. J. Burgess, Electrochim. Acta 53 (2008) 6759-6767.

(11) Y. Chen, X. Yang, B. Jin, L. Guo, L. Zheng, X. Xia, J. Phys. Chem. C 113 (2009) 4515-4521.

(12) A. M. Luque, W. H. Mulder, J. J. Calvente, A. Cuesta, R. Andreu, Anal. Chem. 84 (2012) 5778-5786.

(13) C. Ma, J. M. Harris, Langmuir 27 (2011) 3527-3533.

(14) K. Sugihara, K. Shimazu, K. Uosaki, Langmuir 16 (2000) 7101-7105.

(15) N. Goutev, M. Futamata, Appl. Spectrosc. 57 (2003) 506-513.

(16) M. Futamata, J. Electroanal. Chem. 550-551 (2003) 93-103.

(17) C. P. Smith, H. S. White, Langmuir 9 (1993) 1-3.

(18) W. R. Fawcett, M. Fedurco, Z. Kovacova, Langmuir 10 (1994) 2403-2408.

(19) R. Andreu, W. R. Fawcett, J. Phys. Chem. 98 (1994) 12753-12758.

(20) C. Vaz-Domínguez, M. Pita, A.L. de Lacey, S. Shleev, A. Cuesta, J. Phys. Chem. C 116 (2012) 16532-16540.

(21) A. Krezel, W. Bal, J. Inorg. Biochem. 98 (2004) 161-166.

(22) C. Méthivier, B. Beccard, C. M. Pradier, Langmuir 19 (2003) 8807-8812.

(23) O. Gershevitz, A. Osnis, C. N. Sukenik, Israel J. Chem. 45 (2005) 321-336.

(24) D. Aureau, F. Ozanam, P. Allongue, J. N. Chazalviel, Langmuir 24 (2008) 9440-9448.

(25) D. L. Allara, J. D. Swallen, J. Phys. Chem. 86 (1982) 2700-2704.

(26) D. L. Allara, R. G. Nuzzo, Langmuir 1 (1985) 52-66.

(27) S. Ye, Y. Sato, K. Uosaki, Langmuir 13 (1997) 3157-3161.

(28) S. M. Rosendahl, I. J. Burgess, Electrochim. Acta 56 (2011) 4361-4368.

(29) M. Tominaga, S. Maetsu, A. Kubo, I. Taniguchi, J. Electroanal. Chem. 603 (2007) 203-211.

(30) P. Ramirez, A. Granero, R. Andreu, A. Cuesta, W. H. Mulder, J. J. Calvente, Electrochem. Commun. 10 (2008) 1548-1550.

(31) S. E. Creager, J. Clarke, Langmuir 10 (1994) 3675-3683.

(31) M. Borkovec, Langmuir 13 (1997) 2608-2613.